This is a post-peer reviewed version of the manuscript published in:

RSC Advances, 2014, Volume 4, Pages 45168-45173

(DOI: 10.1039/c4ra07451c)

Journal Name

RSCPublishing

ARTICLE

Spectroelectrochemical synthesis of gold nanoparticles using cyclic voltammetry in presence of a protective agent

Cite this: DOI: 10.1039/xoxxoooooox

Received ooth January 2012,
Accepted ooth January 2012

DOI: 10.1039/xoxxoooooox

www.rsc.org/

C. Fernandez-Blanco,[a] A. Heras,[a] V. Ruiz[b] and A. Colina*[a]

Modification of electrodes with metal nanoparticles (NPs) is attracting intense interest because the widespread applications of these electrodes as sensors in electroanalysis. In the present study, we have analysed the electrodeposition of gold nanoparticles (Au NPs) on a platinum electrode in presence of polyvinylpyrrolidone using UV/Vis spectroelectrochemistry, which allows us to obtain *in-situ* evidences on the kind of nanoparticles deposited on the electrode. Under the selected experimental conditions, it has been possible to understand the reaction pathway for the synthesis of Au NPs in a voltammetry experiment. We establish that generation of NPs of a specific size is dramatically favoured during the different oxidation and reduction processes. Experiments with and without protective agent revealed that NPs generation is favoured since the first cycle when a protective agent is present in solution.

Introduction

Synthesis of noble-metal nanoparticles (NPs) has received significant attention in recent years.[1–4] The ability to generate NPs with controlled size and shape is very important to advance in many areas of science and technology. In fact, scientists are beginning to understand the complex physics that leads to the generation of NPs with controlled size and shape.[5–7] In general, the chemical synthesis route is more developed than the electrochemical one, as it allows better control of the final type of NPs.[5,8,9] However, a number of studies have shown that it is also possible to control Au NPs morphology using electrochemistry,[10–16] although a lot of them use a gold sacrificial anode like source of gold ions. [13–15] Electrochemical synthesis offers important advantages such as the production of NPs with high purity.[3] With chemical synthesis is possible to obtain well-defined NPs controlling the ratio between the reductive agent, gold precursor and protective agent.[5,8,9] On the other hand, electrochemical synthesis is very interesting to understand the mechanism of NPs generation because it is possible to control easily the potential at which the reaction takes place.

In the case of the electrochemical synthesis, the reaction mechanism can be better understood when *in-situ* characterization techniques are coupled to electrochemistry to provide more information about the process that is taking place.[17–21] Here electrochemistry is combined with UV/Vis absorption spectroscopy to follow the formation of Au NPs. UV/Vis spectroelectrochemistry provides mechanistic information on Au NPs synthesis because the electrochemical process can be easily followed by observing gold characteristic plasmon band.[2,22] Recently, we have demonstrated that a multipulse technique yields monodisperse spherical Au NPs.[19] This method was based on the application of several consecutive oxidation/reduction steps. In order to understand better the electrochemical process, here we have developed a new synthesis route based on cyclic voltammetry, where reduction and oxidation potentials are alternated dynamically.

In this work, we have studied Au NP electrodeposition on a platinum electrode by UV/Vis spectroelectrochemistry in presence of polyvinylpyrrolidone (PVP), one of the main protective agents used in metal nanoparticle synthesis.[1,23] Protective agents are generally used to avoid NPs agglomeration. In many cases, these agents play a crucial role

in the control of NPs size and shape based on the use of multifunctional ligands, polymers and surfactants.[24,25] PVP is a homopolymer with long and soft polyvinyl chain, whose monomer has a hydrophilic cyclic amide group. The nitrogen and oxygen atoms of this polar group have a strong affinity for transition metal and their metal clusters.[26]

The main goal of our work is to demonstrate that UV/Vis absorption spectroelectrochemistry helps to understand the process taking place during the different oxidation and reduction steps, providing important information about the mechanism of NPs generation.

Results and discussion

Au NPs were synthesized employing different experimental conditions. Initially, Au NPs formation was studied employing different supporting electrolytes as $HClO_4$, HCl or KCl obtaining better results using HCl or KCl due to a special stabilization of NPs with the use of Cl^- anion. PVP was added for getting a better NPs stabilization and different concentrations of gold salt were employed, obtaining NPs with different plasmon band depending on these factors. In the literature can be found examples of Au NPs synthesis using a unique reduction potential pulse[27], but in our case it was not possible to obtain monodisperse NPs. On the contrary, NPs with a more defined plasmon band were obtained when consecutive oxidation and reduction potentials were applied. Therefore, we thought in cyclic voltammetry as a method to understand the mechanism of generation of NPs when consecutive oxidation and reduction potentials are gradually applied to the electrode.

Different experiments were performed to select the oxidation/reduction potential limits. We began applying high oxidation potentials as vertex potentials, but values higher than +0.95 V do not provide NPs with a narrow plasmon band. In some cases, even no NPs were formed because the complete oxidation of the NPs on the electrode surface takes place. From the previous results, the next experimental conditions were selected to study the mechanism of generation of NPs: the electrosynthesis of Au NPs was carried out by cyclic voltammetry (CV) scanning the potential from +0.40 V to +0.95 V and back to +0.25 V for 20 cycles at a scan rate of 250 mV·s-1 in $2 \cdot 10^{-3}$ M $HAuCl_4$, using 0.5 M KCl solution as supporting electrolyte and in presence of 20 g·dm-3 PVP K30 as protecting agent against NPs agglomeration. The initial potential of +0.40 V was selected because it is low enough to form the initial gold clusters on the electrode surface. The reduction current indicates that reduction of $AuCl_4^-$ is taking place and an increase of absorbance demonstrates that gold clusters are being formed on the electrode surface. These clusters should be very small (<2 nm) because no plasmon band is observed. Potential was scanned up to +0.95 V because it is high enough to oxidize electrogenerated Au NPs without removing all the electrodeposited gold. Finally, the potential is changed back to a value of +0.25 V where gold in solution can be reduced to yield metal NPs. Finally, scan rate was high enough to minimize diffusion of oxidized gold species from the electrode surface before its reduction.

Fig. 1a shows the voltammetric response for Au NPs electrosynthesis. At the beginning of the synthesis, a fast reduction of $AuCl_4^-$ anion is observed, corresponding to formation of the first nuclei of Au NPs on the electrode surface. The first cycle is clearly different, but the voltammogram reaches a stationary waveform when the experiment goes on. A broad reduction peak around +0.50 V that decreases with the number of cycles and the onset potential for the oxidation peak around +0.90 V is observed. The absence of additional oxidation or reduction features indicates that not enough information about the electrodeposition mechanism is obtained only from the electrochemical signal.

Spectroscopy data, simultaneously recorded with the electrochemical signal, allow us to obtain complementary information. Fig. 1b shows the spectra measured at +0.25 V at the end of the 5th, 10th, 15th and 20th cycle. A plasmon band centred at 570 nm is observed, which grows from cycle to cycle, confirming that Au NPs are deposited on the Pt electrode. This band is broader and red-shifted with respect to the plasmon band of individual NPs.[28,29] Au NPs usually exhibit a band around 520 nm that red-shifts when a high density of NPs are deposited on the electrode surface because of the electromagnetic properties of interacting metal nanoparticles in close mutual proximity.[30] The interaction energy (coupling of two nearby oscillators) is sufficiently strong for nearly adjacent NPs to shift their resonant frequencies, resulting in red-shifting relative to the resonance of each individual NP.[30–33]

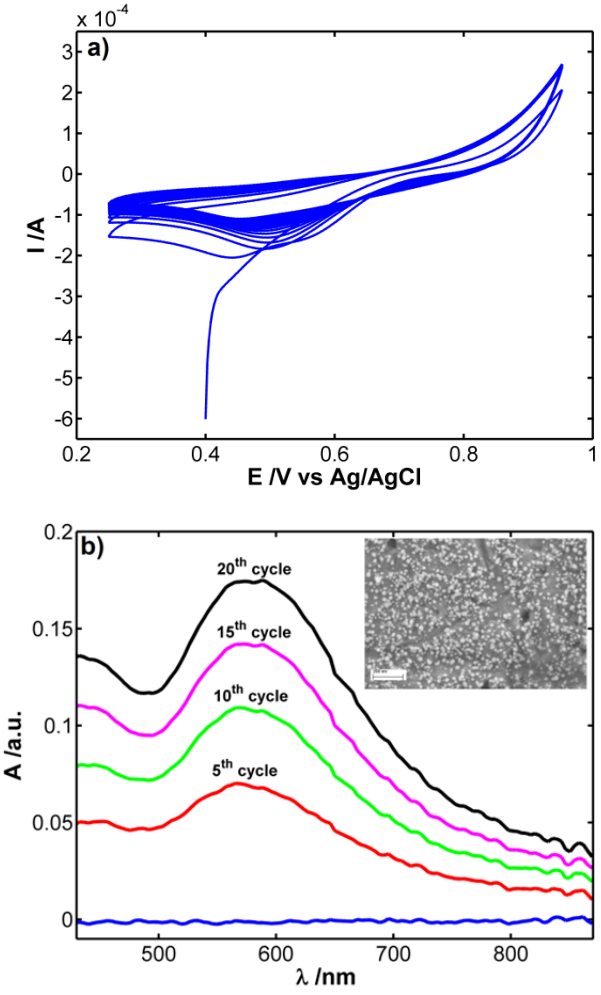

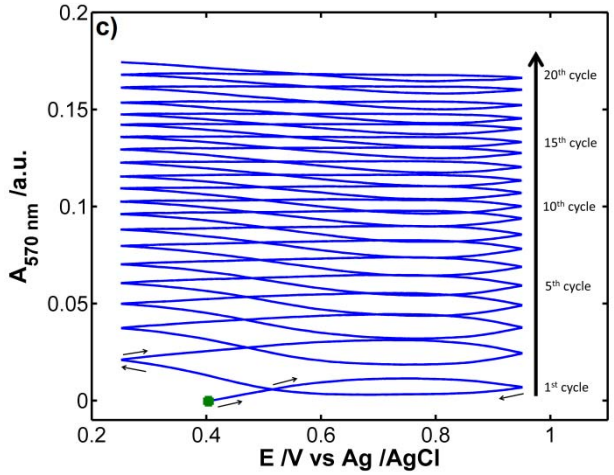

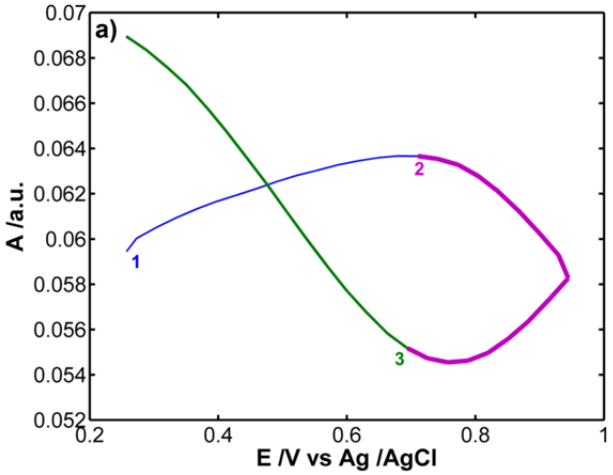

Fig. 1 a) Voltammogram measured during Au NPs electrosynthesis in $HAuCl_4$ $2{\cdot}10^{-3}$ M using 0.5 M KCl solution as supporting electrolyte in presence of 20 $g{\cdot}dm^{-3}$ PVP K30 as protecting agent. Scan rate: 250 $mV{\cdot}s^{-1}$, starting potential: +0.40 V, first vertex potential: +0.95 V, second vertex potential: +0.25 V, number of cycles: 20. b) Spectra recorded at +0.25 V at the end of the 5th, 10th, 15th and 20th cycle. Inset: FE-SEM image of the Au NPs deposited. c) Evolution of absorbance at 570 nm with potential during the experiment. ● Indicates the beginning of the experiment.

Thus, the spectrum corresponding to the end of the electrosynthesis provides information on the kind of NPs deposited on the electrode. This information can be compared with SEM image in Fig. 1b inset (more SEM images, Fig S1-S6, in supplementary information)

From the SEM image a diameter of 20 ± 2 nm is estimated for the Au NPs deposited on the electrode surface. The plasmon band is wider than expected, meaning that there is a high density of Au NPs on the electrode as can be observed in Fig. 1b inset. Dynamic spectroelectrochemical techniques with high resolution time (acquisition of one spectrum every 25 ms) allow us, first, to observe the generation of new compounds and, second, to monitor the kinetics of the process. Fig. 1c shows the absorbance *vs.* potential plot at the absorbance maximum wavelength, 570 nm. Two main regions are observed, one at potentials lower than +0.50 V and another one at potentials higher than +0.70 V. In the first region, the absorbance increases so the reduction of oxidized gold is taking place, indicating the generation of new Au NPs.

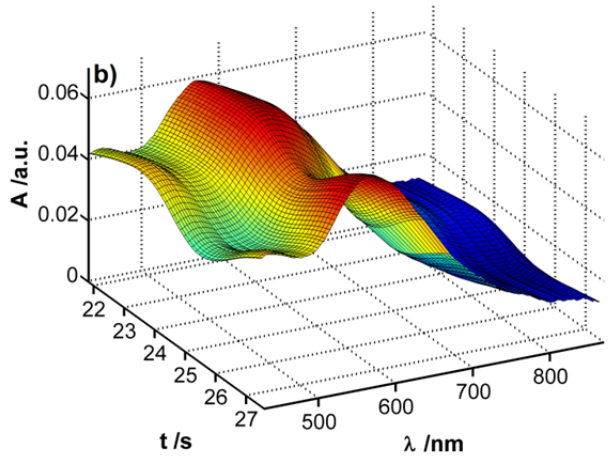

Fig 2 a) Evolution of absorbance at 570 nm with potential recorded during the 5th cycle, showing the different segments where the reference spectrum is taken, marked with numbers. b) Full spectra recorded during the 5th cycle.

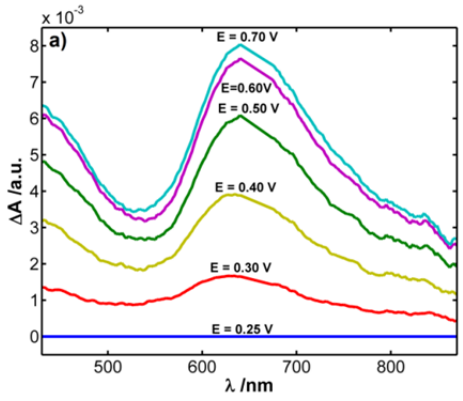

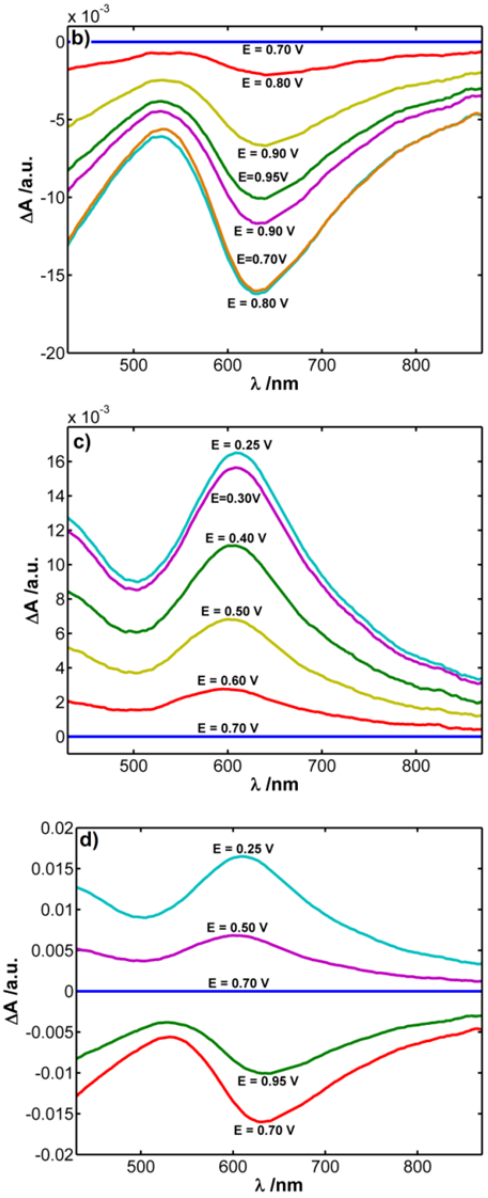

Fig 3 Evolution of absorbance during the different potential segments taking as reference spectrum the first point of the segment in the 5th cycle. a) From +0.25 V to +0.70 V, b) from +0.70 V to +0.95 V and from +0.95 V to +0.70 V, c) from +0.70 V to +0.25 V. d) Evolution of the absorbance for the 2nd segment (negative increments) and 3rd segment (positive increments).

As can be seen, the increase of absorbance at 570 nm starts concomitantly with the broad reduction peak around +0.50 V. In the second region, at high potential values, belonging to the end of the studied range, NPs oxidation takes place leading to a small absorbance decrease but without the total dissolution of NPs from the surface.

Along the experiment, a linear shifting of 8 nm of the maximum of the plasmon band with the number of cycles is observed (Figure S7, supplementary information), indicating that NPs size increases cycle by cycle. SEM images (Fig S8-S12, supplementary information) demonstrate that Au NPs size was 13 nm in the 8th cycle and increases up to 20 nm in the 20th cycle.

To shed more light on the reaction pathway, a careful analysis of the spectroscopic signals at different potentials during the different cycles is needed. Fifth cycle has been selected as representative to illustrate the evolution of the overall electrodeposition process. Fig. 2a shows the voltabsorptogram at the maximum of the Au NPs plasmon band, denoting the different segments in which we have divided the 5th cycle. We have divided each cycle in 3 different segments: (1) from +0.25 V to +0.70 V, blue line, (2) from +0.70 V to +0.95 V, returning to +0.70 V, magenta line and (3) from +0.70 V to +0.25 V, green line.

Fig. 2b shows the time-resolved evolution of the spectra during the three segments. As can be expected, during the first segment, from +0.25 V to +0.70 V, absorbance grows in this potential region due to the generation of NPs. The other two segments are also very informative. During the second segment absorbance decreases because some Au NPs are partially dissolved, and finally during the third segment, absorbance grows again due to the generation of new NPs, but in this case NPs formation is faster than in the first segment as evidences the higher slope of the absorbance growth. Although the process is described in a rough mode, it can be observed in more detail if the increments of absorbance that are taking place during each segment are studied.

Numbers in Fig. 2a show the potential of the spectra took as reference to calculate the increments of absorbance for each segment shown in Fig. 3. Thus, Fig 3 represents the spectroscopic increments of absorbance at different potential (shown in legend) taking as reference spectrum the first one at the beginning of each segment. We wish to remark that the figures show spectral changes during each segment, recalculating absorbance values with respect to a different reference spectrum. Change of reference spectrum provokes an "apparent" blue-shifting of the plasmon band because the new reference spectrum exhibits a strong absorption (plasmon band) centred at 570 nm. We are not observing the absolute absorbance but the increment of absorbance respect to a new reference spectra, that is to say, we are observing how the plasmon band is modified in a range of potential. Absorbance respect the initial reference spectrum is centred at 570 nn. From the evolution of these recalculated spectra it is possible to explain the mechanism of Au NPs generation in presence of PVP.

During the 5th cycle an increase of ΔA is observed in the 1st segment, with a clear plasmon band that grows (Fig. 3a). Gold deposited on the electrode is partially redissolved at potentials higher than +0.70 V (Fig. 3b), as can be deduced from the decrease of ΔA. This behaviour is observed for all potential cycles registered. Gold is redissolved from NPs large enough to exhibit plasmon band in presence of PVP. During the 3rd segment, the plasmon band increases indicating that more Au NPs are being generated (Fig. 3c), and a very well defined plasmon band is observed. Fig. 3d shows ΔA for the 2nd and the 3rd segment plotted in the same figure. In this way, it is easily deduced that, Au NPs which are disappearing during the oxidation have a plasmon band centred at a higher wavelength than Au NPs that are being formed in the 3rd segment. In the 2nd segment, dissolved NPs shows a maximum centred at 630 nm, meanwhile, the band that is observed in the 3rd segment shows a maximum centred at 605 nm. Moreover, the bandwidth of the plasmon band for the case of the 2nd segment is wider than the one for the 3rd segment. This behaviour can be explained in terms of consumption of bigger Au NPs to form smaller NPs, all of them with a similar size that provokes a narrowing of the plasmon band. This spectra evolution within the different segments is observed for all potential cycles performed in the

voltammetric experiment. Therefore, spectroelectrochemistry indicates that the generation of a specific size is favoured during the deposition of redissolved gold. The consecutive oxidation-reduction process implies an effect similar to the aging process observed in precipitation. Aging for Au NPs formed by repeated oxidations-reductions can be understood as an irreversible structural change occurring during the formation of NPs by a recrystallization or transformation of a metastable modification into a more stable form. Therefore, under these experimental conditions, a high density of NPs with a plasmon band centred at 570 nm are preferentially deposited.

Au NPs have also been successfully synthesized in absence of protective agent to demonstrate the role of PVP in the synthesis. The electrosynthesis of these Au NPs has also been carried out by cyclic voltammetry in conditions comparable to those for the synthesis described in Fig. 1. The solution in this case was $2 \cdot 10^{-3}$ M $HAuCl_4$ with 0.5 M KCl as supporting electrolyte. Again, the potential was scanned from +0.40 V to +0.95 V and back to +0.25 V for 20 cycles at a scan rate of 250 $mV \cdot s^{-1}$ Fig. 4a shows the cyclic voltammogram corresponding to Au NPs electrosynthesis under these new experimental conditions. As in the previous case, a fast reduction of $AuCl_4^-$ can be seen just after applying the initial potential of +0.40 V, with the first cycle being clearly different than the other ones. Two reduction peaks (around +0.75 V and +0.50 V) and one oxidation peak (around +0.90 V) that grows from the first to the eighth cycle are noted. However, it is very difficult to extract specific information about the reaction mechanism from the electrical signal alone.

Again, spectroscopy data provides suitable information about the generation of NPs. Fig. 4b shows the evolution of spectra at +0.25 V at the end of the 5th, 10th, 15th and 20th cycle. As can be seen, absorbance increases cycle by cycle and a plasmon band centred at 555 nm emerges only when Au NPs are generated. During the first cycles no plasmon band is observed, being the maximum of absorbance centred at 460 nm suggesting that very few and/or small nanoparticles (< 2nm) are deposited. From the 6th cycle onwards, a plasmon band is clearly visible, indicating that Au NPs are being electrosynthetized although no stabilizer was added. In this part of the experiment, the maximum of absorbance is drastically shifted from 460 to 550 nm corroborating the conclusion that Au NPs are generated. The voltabsorptogram at the wavelength of the plasmon band, λ = 555 nm, is shown in Fig. 4c.

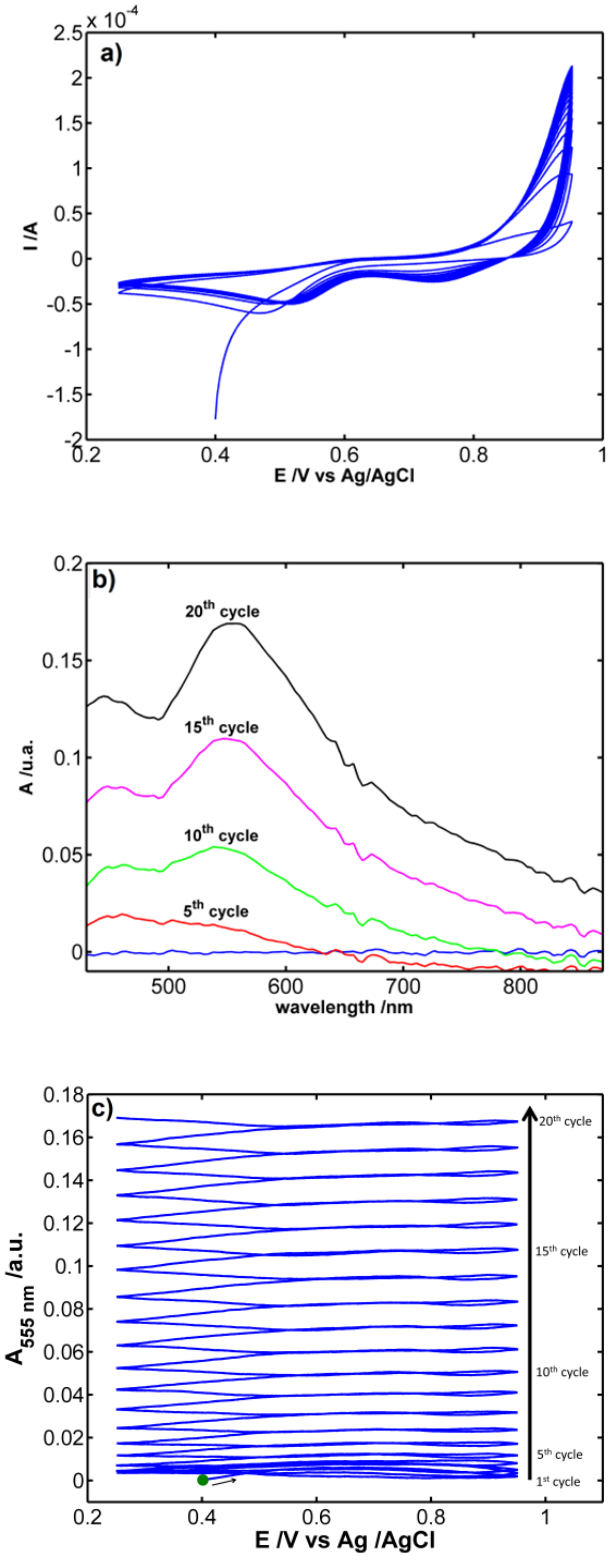

Fig. 4. a) Voltammogram measured during Au NP electrosynthesis in absence of PVP. Scan rate: 250 $mV \cdot s^{-1}$, starting potential: +0.40 V, first vertex potential: +0.95 V, second vertex potential: +0.25 V, number of cycles: 20. b) Spectra recorded at +0.25 V at the end of the 5th, 10th, 15th and 20th cycle. c) Evolution of absorbance at 555 nm with potential during the experiment.

Absorbance increases slowly during the first five cycles, while from the 6th cycle onwards an almost linear growth with the number of cycles at +0.25 V is observed. The values of absorbance at the maximum of the plasmon band at +0.25 V for the 20 registered cycles are completely different with and without PVP, Fig. S13. This fact reveals that the mechanism of generation of Au NP strongly depends on the presence or absence of this protective agent. When PVP is present in solution, NPs generation is favoured since the first cycle, however in absence of PVP is much more complicated to synthesize monodisperse Au NPs.

From the final spectra it can be conclude that NPs are formed in presence or in absence of PVP, although the reaction pathways are clearly different, highlighting the importance of *in-situ* studies of the electrodeposition process to understand how the intermediate states of the NPs allow us to control the final product of the electrosynthesis.

Experimental

All reagents were of analytical grade and were used as received: hydrogen tetrachloroaurate (III) trihydrate ($HAuCl_4 \cdot 3H_2O$) (Acros Organics), polyvinylpyrrolidone, PVP K30 (Fluka), potassium chloride, KCl (Panreac).

Aqueous solutions were prepared using high-quality water (resistivity of 18.2 MΩ·cm, Milli-Q gradient A10 system, Millipore).

All spectroelectrochemical experiments were carried out at room temperature using a potentiostat/galvanostat AUTOLAB PGSTAT 10 electrochemical system with GPES software, coupled with a QE65000 Fiber Optic Spectrometer (Ocean Optics) made up of a 1044×64 element diode array. The light beam, supplied by a deuterium-halogen light source (Avalight-DH-S, Avantes) was both conducted to and collected from the spectroelectrochemical cell by a reflection probe (RP-200-7-UV/Vis, Ocean Optics). The reflection probe, a bifurcated bundle consisting of six 200-µm illumination fibers around one central read fiber, was placed in a home-made cell, facing the surface of the Pt electrode at a distance of approximately 1.5 mm. In this way, the beam is incident perpendicularly to the electrode surface and the reflected light (which samples a spot of approximately 1 mm^2) is collected by the central read fiber of the reflection probe and conducted to the spectrometer. A standard three-electrode cell was used in all the experiments, consisting of a commercial Pt working electrode (CHI), a Pt wire as auxiliary electrode and a homemade Ag/AgCl/KCl (3 M) as reference electrode

Before gold deposition, the platinum electrode was polished to a mirror finish using alumina slurries with different powder size down to 0.05 µm. After each polishing, the electrode was thoroughly rinsed with water and sonicated in ultrapure water in an ultrasonic bath for 30 min in order to remove any adsorbed substances on the electrode surface. Pt working electrode was not electrochemically polished.

The electrode surface was examined with a ZEISS Ultra Plus field-emission scanning electron microscope (FE-SEM).

Conclusions

In summary, a fine control of the experimental conditions has allowed us to synthesize Au NPs in presence of protective agent. UV/Vis absorption spectroelectrochemistry helps to study the reaction pathway because in-situ spectroscopic data are obtained during the electrochemistry experiment.

Cyclic voltammetry in a suitable potential window drives consecutive oxidation and reduction reactions that yield to a specific type of NPs. The final spectra can be compared with the SEM image and it shows that monodisperse and spherical Au NPs have been electrosynthetized. The reaction mechanism shows that, to reach this kind of monodisperse NPs, bigger NPs are consumed during the oxidation potentials to form smaller and more stable NPs during the reduction potentials. Thus, formation of NPs with a specific size is favoured during the electrosynthesis. The mechanism of synthesis of Au NP strongly depends on the presence or absence of a protective agent.

Acknowledgements

The financial support made available by the Junta de Castilla y León (GR71, BU349-U13), Ministerio de Economía y Competitividad (CTQ2010-17127, V. R. Programa Ramón y Cajal) and the Academy of Finland is gratefully acknowledged. C. F-B. thanks Ministerio de Educación, Cultura y Deporte for a predoctoral FPU fellowship.

Notes and references

[a] Department of Chemistry, Universidad de Burgos, Pza. Misael Bañuelos s/n, E-09001 Burgos, Spain. E-mail: acolina@ubu.es

[b] New Materials Department. CIDETEC-IK4 - Centro de Tecnologías Electroquímicas. Parque Tecnológico de San Sebastián. Paseo Miramón, 196 E-20009 Donostia - San Sebastián, Spain

† DOI: 10.1039/b000000x/

1. R. Sardar, A. M. Funston, P. Mulvaney, and R. W. Murray, *Langmuir*, 2009, **25**, 13840–13851.
2. M. C. Daniel and D. Astruc, *Chem. Rev.*, 2004, **104**, 293–346.
3. J. Park, J. Joo, S. G. Kwon, Y. Jang, and T. Hyeon, *Angew. Chemie Int. Ed.*, 2007, **46**, 4630 – 4660.
4. S. Eustis and M. A. El-Sayed, *Chem. Soc. Rev.*, 2006, **35**, 209–17.
5. Y. Xia, Y. Xiong, B. Lim, and S. E. Skrabalak, *Angew. Chem. Int. Ed.*, 2009, **48**, 60–103.
6. M. Grzelczak, J. Pérez-Juste, P. Mulvaney, and L. M. Liz-Marzán, *Chem. Soc. Rev.*, 2008, **37**, 1783–91.
7. C.-H. Cui, H.-H. Li, and S.-H. Yu, *Chem. Commun.*, 2010, **46**, 940–2.
8. D. T. Nguyen, D.-J. Kim, and K.-S. Kim, *Micron*, 2011, **42**, 207–227.
9. J. Kimling, M. Maier, B. Okenve, V. Kotaidis, H. Ballot, and a Plech, *J. Phys. Chem. B*, 2006, **110**, 15700–7.
10. U. S. Mohanty, *J. Appl. Electrochem.*, 2010, **41**, 257–270.
11. J.-J. Feng, A.-Q. Li, Z. Lei, and A.-J. Wang, *ACS Appl. Mater. Interfaces*, 2012, **4**, 2570–2576.
12. Y. Hu, Y. Song, Y. Wang, and J. Di, *Thin Solid Films*, 2011, **519**, 6605–6609.
13. S. Chang, C. Shih, C. Chen, W. Lai, and C. R. C. Wang, *Langmuir*, 1999, **15**, 701–709.

14. C.-J. Huang, P.-H. Chiu, Y.-H. Wang, W. R. Chen, and T. H. Meen, *J. Electrochem. Soc.*, 2006, **153**, 129–133.
15. C.-J. Huang, Y.-H. Wang, P.-H. Chiu, M.-C. Shih, and T.-H. Meen, *Mater. Lett.*, 2006, **60**, 1896–1900.
16. S.-P. Tung, T.-K. Huang, C.-Y. Lee, and H.-T. Chiu, *RSC Adv.*, 2012, **2**, 1068.
17. C. Zanardi, F. Terzi, L. Pigani, A. Heras, A. Colina, J. Lopez-Palacios, and R. Seeber, *Electrochim. Acta*, 2008, **53**, 3916–3923.
18. E. Ventosa, A. Colina, A. Heras, A. Martínez, O. Orcajo, V. Ruiz, and J. López-Palacios, *Electrochim. Acta*, 2008, **53**, 4219–4227.
19. C. Fernández-Blanco, A. Colina, A. Heras, V. Ruiz, and J. López-Palacios, *Electrochem. Commun.*, 2012, **18**, 8–11.
20. W. Kaim and J. Fiedler, *Chem. Soc. Rev.*, 2009, **38**, 3373–82.
21. C. Renault, K. D. Harris, M. J. Brett, V. Balland, and B. Limoges, *Chem. Commun.*, 2011, **47**, 1863–5.
22. K. Rahme, L. Chen, R. G. Hobbs, M. A. Morris, C. O'Driscoll, and J. D. Holmes, *RSC Adv.*, 2013, **3**, 6085.
23. C. E. Hoppe, M. Lazzari, I. Pardiñas-Blanco, and M. A. López-Quintela, *Langmuir*, 2006, **22**, 7027–7034.
24. T. K. Sau and A. L. Rogach, *Adv. Mater.*, 2010, **22**, 1781–1804.
25. F. Dumur, A. Guerlin, E. Dumas, D. Bertin, D. Gigmes, and C. R. Mayer, *Gold Bull.*, 2011, **44**, 119–137.
26. S. Huang, H. Ma, X. Zhang, F. Yong, X. Feng, W. Pan, X. Wang, Y. Wang, and S. Chen, *J. Phys. Chem. B*, 2005, **109**, 19823–19830.
27. C. Wang, R. Yuan, Y. Chai, S. Chen, F. Hu, and M. Zhang, *Anal. Chim. Acta*, 2012, **741**, 15–20.
28. J. Turkevich, G. Garton, and P. C. Stevenson, *J. Colloid Sci.*, 1954, **9**, 26–35.
29. S. Link and M. A. El-Sayed, *J. Phys. Chem. B*, 1999, **103**, 4212–4217.
30. N. J. Halas, S. Lal, W.-S. Chang, S. Link, and P. Nordlander, *Chem. Rev.*, 2011, **111**, 3913–61.
31. P. K. Aravind, A. Nitzan, and H. Metiu, *Surf. Sci.*, 1981, **110**, 189–204.
32. M. Quinten, U. Kreibig, D. Schönauer, and L. Genzel, *Surf. Sci.*, 1985, **156**, 741–750.
33. L. M. Liz-Marzán, *Langmuir*, 2006, **22**, 32–41.